Photoemission studies of the conduction band filling in $Ti_{1.05}S_2$ and Cs-intercalated TiS_2 and $ZrSe_2$

1996 J. Phys.: Condens. Matter 8 1229

(http://iopscience.iop.org/0953-8984/8/9/013)

J. Phys.: Condens. Matter **8** (1996) 1229–1234. Printed in the UK

Photoemission studies of the conduction band filling in $Ti_{1.05}S_2$ and Cs-intercalated TiS_2 and $ZrSe_2$

H I Starnberg†, H E Brauer† and H P Hughes‡

† Department of Physics, Chalmers University of Technology and Göteborg University, S-412 96 Göteborg, Sweden

‡ Cavendish Laboratory, Madingley Road, Cambridge CB3 0HE, UK

Received 23 October 1995, in final form 27 November 1995

Abstract. We have used photoelectron spectroscopy to study the filling of conduction band states of the layered semiconductors TiS_2 and $ZrSe_2$ as they are intercalated by Cs. Comparison is also made with 'self-intercalated' $Ti_{1.05}S_2$. Even in the pure samples, occupied conduction band states due to excess Ti/Zr are found, but this occupancy is greatly increased by Cs intercalation. The stoichiometries are estimated from the extent in $\boldsymbol{k}$-space of the occupied bands. A weak structure just below the conduction band minimum of $Ti_{1.05}S_2$ is tentatively attributed to localized defect states.

1. Introduction

The layered transition metal dichalcogenides (TMDCs), and the intercalation compounds which are formed as foreign atoms or molecules are inserted between TMDC layers, are of significant interest as model systems for studies of reduced dimensionality and related phenomena [1]. They are also of significant practical interest, e.g. as electrode materials in advanced batteries [2].

A crucial issue in fundamental as well as applied research is the understanding of the intercalation reaction, in which electrons are transferred from the guest species to the host layers. The effect of intercalation is often analysed in terms of the rigid-band model, which assumes that the donated electrons merely increase the filling of the host bands, without further modifications. Although it has been demonstrated that this is not strictly true [3, 4], the model may still be used as a first approximation in many cases.

In this paper we report photoemission results for $Ti_{1.05}S_2$, Cs_xTiS_2 and Cs_xZrSe_2. Unintercalated TiS_2 and $ZrSe_2$, both adopting the 1T-CdI_2 structure, are characterized by filled valence bands primarily of chalcogen p character, and a lowest conduction band of mainly metal d character. As the valence and conduction bands are separated by energy gaps ($\sim$0.2 eV for TiS_2 and $\sim$1.1 eV for $ZrSe_2$), both materials are in principle semiconductors, but in practice they are always degenerately n doped due to inclusion of excess metal. In a photoemission study of TiS_2 samples of varying stoichiometry, Barry *et al* [5] convincingly demonstrated that the additional electrons reside in pockets around the $\bar{M}$ points of the hexagonal surface Brillouin zone (SBZ). Essentially the same behaviour is expected for $ZrSe_2$. We have studied the intercalation-induced occupancy of the Ti 3d and Zr 4d states in some more detail as TiS_2 and $ZrSe_2$, respectively, are intercalated.

In the case of $Ti_{1.05}S_2$ we have also exploited the temperature dependence of the photoemission process to distinguish between direct ($\boldsymbol{k}$-conserving) and non-direct transitions.

0953-8984/96/091229+06$19.50

2. Experimental details

Photoelectron spectra for $Ti_{1.05}S_2$ were measured using He I radiation ($h\nu = 21.22$ eV), while the Cs-intercalation studies, also made by photoelectron spectroscopy, were performed at beamline 41 ($h\nu = 20$–200 eV) of the MAX-lab synchrotron radiation facility in Lund, Sweden. The total energy resolution was typically 0.1 eV in both cases. The crystallographic directions for the samples were determined using LEED.

The unintercalated single-crystal samples, including the non-stoichiometric $Ti_{1.05}S_2$, were grown by the vapour-transport method. The latter sample was actually taken from the same batch as the 'poor-stoichiometry' sample used by Barry *et al* [5], which had a carrier concentration of 3.3×10^{21} cm^{-3} as determined from the Hall coefficient. Clean mirror-like surfaces were obtained by cleavage in UHV.

The Cs-intercalated samples were prepared by UHV deposition of Cs onto clean cleavage planes at room temperature. This procedure has previously been demonstrated to result in spontaneous intercalation [3, 4, 6]. The Cs atoms are highly mobile along the host layers, and apparently their mobility across the host layers, via edges and crystal imperfections, is high enough to allow for rapid intercalation. The details of this process are still largely unknown, but the usefulness of *in situ* intercalation should motivate further studies. In our case, Cs deposition and intercalation were monitored by recording of Cs 4d core-level spectra, which were dominated by the characteristic features of intercalated Cs [4, 6]. Only a small amount of Cs remained at the surface, probably being trapped by impurities. Repeated depositions induced no significant changes in the spectra, which indicates that deposited Cs atoms are rapidly intercalated into the interior of the substrate, without changing the near-surface composition. LEED patterns showed no extra spots after Cs depositions, thus excluding the possibility of formation of Cs superlattices at room temperature.

3. Results and discussion

3.1. $Ti_{1.05}S_2$

Since the excess Ti occupies interlayer sites, the non-stochiometric TiS_2 is also referred to as 'self-intercalated'. Figure 1 shows energy distribution curves (EDCs) measured at emission polar angles $\theta = 10^\circ$ and 35° in the $\bar{\Gamma}\bar{M}$ azimuthal direction. There are two peaks, labelled A and B, visible in the energy range just below the Fermi level E_F. The intensity of peak A goes through a strong maximum for angles corresponding to emission from states close to $\bar{M}$ in the SBZ, and for these angles peak B is merely seen as a shoulder. This angular dependence clearly identifies peak A as due to transitions from occupied Ti 3d pockets around $\bar{M}$.

To obtain further information about the nature of these two peaks, we have also studied their temperature dependence. Although the theory of such temperature effects is very complex and far from complete, one may exploit the fact that the intensities of direct ($\boldsymbol{k}$-conserving) transitions are reduced by a Debye–Waller factor, while the intensities of indirect transitions generally increase with temperature [7, 8]; emission from localized states, on the other hand, tends to be less dependent on temperature. Figure 1(c) shows a thermal difference spectrum, obtained by subtraction of an EDC measured at elevated temperature (120 °C) from the corresponding room temperature EDC (both measured for $\theta = 35^\circ$). In this kind of difference spectrum, direct transitions will result in peaks, while indirect transitions should produce valleys. Of the two features, A shows up as a sharp peak on a relatively flat background, while B, seen only as a shoulder in the room temperature EDC,

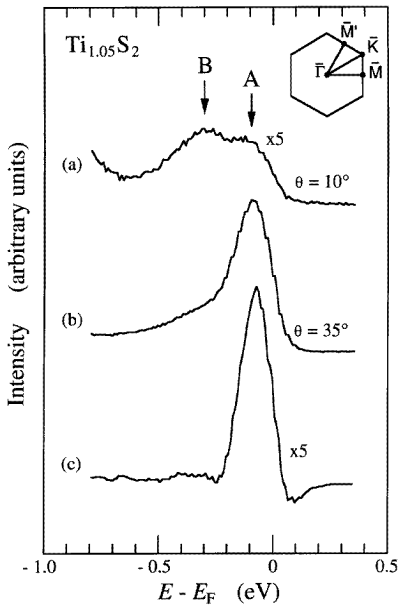

Figure 1. Ti 3d features of $Ti_{1.05}S_2$ as measured in the $\bar{\Gamma}\bar{M}$ azimuth with $h\nu = 21.22$ eV. (a) $\theta = 10^\circ$; (b) $\theta = 35^\circ$; (c) the thermal difference spectrum for $\theta = 35^\circ$. Inset: the surface Brillouin zone (SBZ).

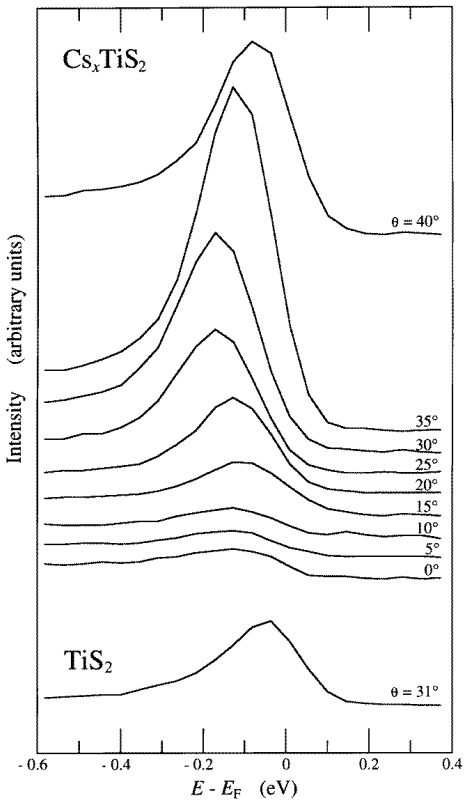

Figure 2. Ti 3d features of Cs_xTiS_2 as measured for different emission angles in the $\bar{\Gamma}\bar{M}$ azimuth with $h\nu = 24$ eV. The $\theta = 31^\circ$ EDC for the sample prior to intercalation is shown at the bottom, for comparison.

is almost invisible in the difference spectrum. This indicates that peak A is dominated by direct transitions, while B is due to localized states rather than band states.

Our observation of two Ti 3d peaks, of which only one behaves like a typical direct-transition peak, provides strong evidence for the existence of localized defect states in this kind of system, as previously suggested by Schärli *et al* [9].

3.2. Cs_xTiS_2

Figure 2 shows a series of EDCs from Cs_xTiS_2, measured with $h\nu = 24$ eV, for different emission angles θ in the $\bar{\Gamma}\bar{M}$ azimuthal direction. At the bottom is shown the corresponding EDC for the unintercalated sample for $\theta = 31^\circ$ ($k_\parallel$ close to the $\bar{M}$ point). On comparison, it is obvious that the occupation of the Ti 3d band is increased greatly upon intercalation with Cs. The Ti 3d feature attributed to defect states in the self-intercalated $Ti_{1.05}S_2$ was also observed (for small θ, not shown), but it was much weaker as the TiS_2 sample used here was closer to stoichiometry. The intercalation with Cs did not result in any conspicuous defect features, although weak structures of this type may be hidden in the tail of the main peak.

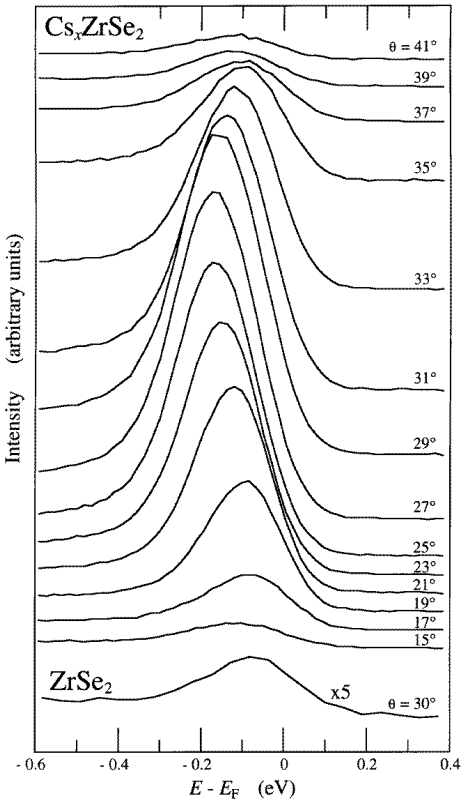

Figure 3. Zr 4d features of Cs_xZrSe_2 as measured for different emission angles in the $\bar{\Gamma}\bar{M}$ azimuth with $h\nu = 24$ eV. The $\theta = 30^\circ$ EDC for the sample prior to intercalation is shown at the bottom, for comparison.

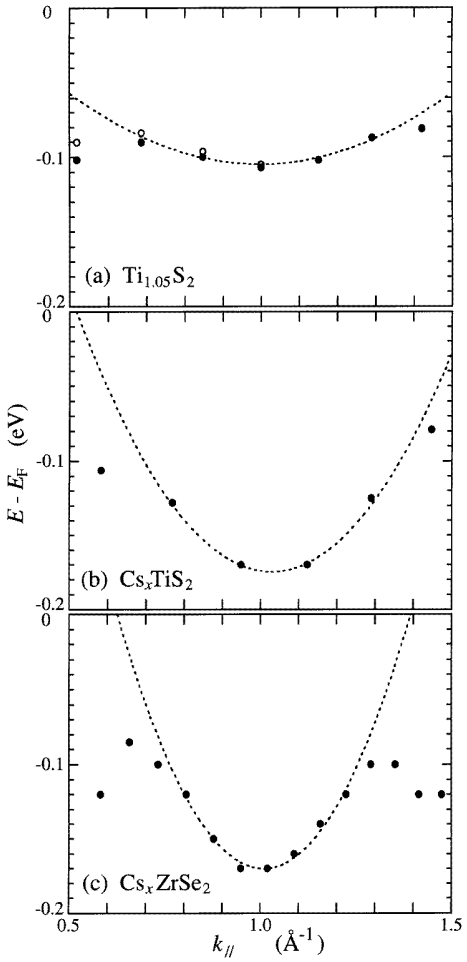

Figure 4. Dispersion of Ti 3d and Zr 4d features along $\bar{\Gamma}\bar{M}$ in (a) $Ti_{1.05}S_2$ (unfilled circles: $\bar{\Gamma}\bar{M}'$ azimuth); (b) Cs_xTiS_2; (c) Cs_xZrSe_2. Dashed lines: numerically fitted parabolic bands.

3.3. Cs_xZrSe_2

Figure 3 shows an analogous series of EDCs for Cs_xZrSe_2, also measured with $h\nu = 24$ eV, for different emission angles θ in the $\bar{\Gamma}\bar{M}$ azimuthal direction. The increased filling of the conduction band upon intercalation is very similar to that observed for Cs/TiS_2. An EDC for the unintercalated sample with $\theta = 30^\circ$ (near $\bar{M}$) is shown for comparison (bottom curve). It is noteworthy that the filling of the conduction band due to excess metal is much smaller for the $ZrSe_2$ than for the TiS_2 sample, i.e. the former is more stoichiometric. No defect features were seen in the $ZrSe_2$ EDCs, which ties in well with the low concentration of excess Zr.

3.4. Dispersions

Since the physical properties of TMDCs and their intercalation complexes are to a large extent determined by the electrons residing in the metal d band close to E_F, it is of fundamental interest to examine these states closely. In figure 4 the measured d-band dispersions for the different systems are summarized. These curves, which show the energies of the d-band peaks versus $k_\parallel$, are obtained by using the relation $k_\parallel = 0.512\sqrt{E_k}\sin\theta$ [10]. One should be aware that the perpendicular component of the wave vector is not determined in the photoemission experiment, but for the materials intercalated with Cs the band structure becomes two dimensional, which eliminates this problem [3, 4]. Another problem is the distortion of EDC peaks close to E_F due to the spectral function being multiplied by the Fermi function. In practice, this means that as a dispersing peak is approaching E_F from below, its apparent position will increasingly lag behind the 'true' position. This kind of distortion is further aggravated by the limited experimental resolution. In principle, the 'true' peak position may be recovered by a deconvolution procedure [11], but in practice it may prove difficult to find unique solutions.

Figure 4(a) shows the dispersion of the $Ti_{1.05}S_2$ direct-transition peak (peak A in figure 1). As the occupied portion of the Ti 3d band is very narrow in energy, the apparent dispersion is strongly suppressed by the Fermi cut-off, although it was partially recovered using a simple fitting scheme involving two gaussians combined with a Fermi function. The fitting procedure was not able to extract the 'true' dispersion, but at least it revealed that the peak is indeed dispersive, which was not detected in earlier studies. Due to the suppressed dispersion, attempts to determine the effective d-band mass from the present data are not meaningful. It should be noted that the range of parabolic dispersion seen in figure 4(a) has a width of $\sim$0.6 Å^{-1} along $\bar{\Gamma}\bar{M}$, in good agreement with the pocket width estimate of Barry *et al* [5]. The observed dispersion is only 20 meV, but the occupied band width, taken to be the distance between the d-band minimum and E_F, is found to be 0.1 eV.

The d-band dispersions of Cs_xTiS_2 and Cs_xZrSe_2, as shown in figures 4(b) and 4(c), are more conspicuous than for $Ti_{1.05}S_2$. Here the experimental points represent the apparent peak positions directly from figures 2 and 3, without any enhancements. The occupied band width in both cases appears to be 0.17 eV. By the fitting of parabolas (dashed lines) the effective masses of the electrons along the $\bar{\Gamma}\bar{M}$ direction were obtained as $11.4m_0$ and $6.5m_0$ for Cs_xTiS_2 and Cs_xZrSe_2, respectively. This is remarkably different from the effective masses obtained from LAPW calculations [4]: $1.8m_0$ and $1.4m_0$, respectively. Even if the experimental effective masses are slightly overestimated due to the influence of the Fermi edge upon the apparent dispersions, it still seems that the d bands have much less dispersion than predicted by the calculations. The reason for this is at present not known, but one may speculate whether correlation effects, which may be strong in narrow d bands, are responsible. To estimate the width in $\boldsymbol{k}$-space of the electron pockets, one may take the ranges of parabolic dispersion as lower limits, while the Fermi level crossings of the extrapolated parabolic bands may provide upper limits. Following this procedure, the electron pocket widths along $\bar{\Gamma}\bar{M}$ are found to be 0.4–0.5 Å^{-1} for Cs_xTiS_2, and 0.3–0.4 Å^{-1} for Cs_xZrSe_2. This in turn corresponds to the following carrier concentrations and stoichiometries: $n = (5.8 \pm 1.2) \times 10^{21}$ cm^{-3}, $x = 0.5 \pm 0.1$ for Cs_xTiS_2; and $n = (3.5 \pm 1.0) \times 10^{21}$ cm^{-3}, $x = 0.35 \pm 0.1$ for Cs_xZrSe_2. To estimate n and x, we assumed the electron pockets to be elliptical cylinders twice as wide along $\bar{\Gamma}\bar{M}$ as in the perpendicular direction. These are the proportions obtained from the LAPW calculations, and although the band masses of the calculated bands were much smaller than the measured ones, we are confident that the calculated ratios of in-plane band masses are reasonable. It

was also assumed that each Cs atom provides one electron to the d-band pockets, which is justified by the fact that the LAPW bands below E_F are essentially modified host bands, with no extra Cs-induced bands appearing [4]. (Above E_F, however, an additional band is seen to hybridize strongly with the upper d bands [12].) Still, the 'modified host bands' may have some Cs 6s character mixed into them, which would mean that a fraction of the electron is still located on the Cs site. It is thus important to recognize that complete transfer to the (modified) host bands is not necessarily equivalent to complete charge transfer in terms of the local density of states.

It is quite clear from the above results that the Cs_xTiS_2 and Cs_xZrSe_2 systems are very similar, while the self-intercalated $Ti_{1.05}S_2$ system differs significantly by having defect states and an energetically much more narrow d band, despite the similar extents in $\boldsymbol{k}$-space of the occupied pockets. This in not unexpected, however, as the interaction of the guest species with the host layers is much stronger for intercalation with 3d transition metals than for intercalation with alkali metals [13]. As a consequence the transition metal ions are not mobile, and the interaction between the host layers (mediated by the intercalated ions) is strengthened, in strong contrast to the 3D-to-2D transition for Cs intercalates [4].

In conclusion, we have through photoemission studies of self-intercalated TiS_2 and Cs-intercalated TiS_2 and $ZrSe_2$ obtained information about the metal d bands which are populated through the intercalation reaction, e.g. that their band masses are 4–7 times larger than calculated. We have also obtained reasonable estimates for the stoichiometries of the samples intercalated with Cs. In particular, for the self-intercalated $Ti_{1.05}S_2$, temperature-dependent measurements reveal evidence for some Ti 3d electrons occupying localized defect states 0.2 eV below the Ti 3d-band minimum. Such defect states, which seem to be associated with non-stoichiometry of the host material, may also be present in the Cs-intercalated systems, although concealed by the intense emission from band states.

Acknowledgments

This work was supported by The Swedish Natural Science Research Council. We would also like to thank the staff at MAX-lab for their skilful assistance

References

[1] Friend R H and Yoffe A D 1987 *Adv. Phys.* **36** 1
[2] Whittingham M S and Ebert L B 1979 *Intercalated Layered Materials* ed F A Lévy (Dordrecht: Reidel)
[3] Starnberg H I, Brauer H E, Holleboom L J and Hughes H P 1993 *Phys. Rev. Lett.* **70** 3111
[4] Brauer H E, Starnberg H I, Holleboom L J and Hughes H P 1995 *Surf. Sci.* **331–333** 419
[5] Barry J J, Hughes H P, Klipstein P C and Friend R H 1983 *J. Phys. C: Solid State Phys.* **16** 393
[6] Pettenkofer C, Jaegermann W, Schellenberger A, Holub-Krappe E, Papageorgopoulos C A, Kamaratos M and Papageorgopoulos A 1992 *Solid State Commun.* **84** 921
[7] Starnberg H I, Ilver L, Nilsson P O and Hughes H P 1993 *Phys. Rev.* B **47** 4714
[8] Starnberg H I and Nilsson P O 1993 *Surf. Sci.* **287/288** 776
[9] Schärli M, Brunner J, Vaterlaus H P and Lévy F 1983 *J. Phys. C: Solid State Phys.* **16** 1527
[10] Hughes H P and Liang W Y 1973 *J. Phys. C: Solid State Phys.* **6** 1684
[11] von der Linden W, Donath M and Dose V 1993 *Phys. Rev. Lett.* **71** 899
[12] Holleboom L J 1994 private communication
[13] Inoue M, Hughes H P and Yoffe A D 1989 *Adv. Phys.* **38** 56